Alkadhum Journal of Science, Vol. 1, No. 2 (2023)

Open Access ISSN: 3005-2386 (Online), ISSN: 3005-2378 (Print)

IRAQI Academic Scientific Journals

Alkadhum Journal of Science (AKJS)

Journal Homepage: https://alkadhum-col.edu.iq/JKCEAS

Alkadhum Journal of Science

Development of an Optical Crystal Fiber Sensor for Early Detection of Tuberculosis

Raed Sattar Jebur* and Raad Hamdan Thaher

Department of Electrical Engineering, University Mustansiriyah, Baghdad, Iraq

Article information

Article history:
Received: October, 22, 2023
Accepted: November, 23, 2023
Available online: December, 14, 2023

Keywords:
Confinement loss,
effective area,
photonic crystal fiber

Corresponding Author:
Raed Sattar Jebur
eeph008@uomustansiriyah.edu.iq

DOI:
https://doi.org/10.61710/akjs.v1i2.59

Abstract

To this day, tuberculosis remains one of the most severe threats to public health on a global scale, which is why there is a pressing need for the development of diagnostic techniques that combine high levels of precision, speed in producing findings, mobility, and risk reduction. This work's planned scope is constructing a photonic crystal fiber sensor with a susceptible non-complex core intended to detect tuberculosis at wavelengths ranging from 1 µm to 2.2 µm. This study introduces an innovative biomedical photonic crystal fiber sensor capable of accurately detecting tuberculosis bacteria across all four strains and effectively distinguishing between them. To carry out numerical studies, the proposed structure uses a technique known the full-vector finite element method (FV-FEM). Compared to earlier biomedical sensors based on photonic crystal fiber, the sensor that has been developed demonstrates an exceptionally high relative sensitivity in detecting various kinds while also displaying a deficient level of loss. The proposed sensor has an effective size of 38 µm2, a sensitivity of 99.9%, and a low confinement loss of 10-11 dB/m. To validate the usefulness of the proposed layout and establish its integrity, a detailed analysis is performed by contrasting the results of this study with the most current research published on photonic crystal fiber.

1. Introduction

Photonic Crystal Fibers (PCFs) are a new type of optical fibers that have holes or air gaps arranged in a pattern along the fiber axis. This characteristic has contributed significantly to its widespread recognition in optics [1]–[3]. The photonic crystal fiber (PCF) composition consists of two main components: the core and the cladding. These components can be modified by employing various shapes and designs [4]. The core of the photonic crystal fiber (PCF) exhibits a higher concentration of light, hence offering a significantly enhanced waveguide for photons compared to conventional fiber optic systems. The photonic crystal fiber (PCF) manipulates the propagation of light by including and controlling air holes at consistent intervals along the length of the fibers. The regulation of light propagation can be achieved by modifying the dimensions of apertures in both the core and cladding. The capacity of blockage to track light within hollow bodies leads to better light penetration and reduced loss, hence enhancing fiber sensitivity [5]. In recent years, researchers have shown great interest in exploring the versatility

of photonic crystal fibers (PCFs) for potential use in various applications, focusing on their use as sensors [6]. Sensing applications encompass biomedical and temperature sensing, chemical detection, pressure detection, gas detection, and more [7]–[13]. Recently, PCFs are very useful and have many benefits that make them popular in sensing uses. As background materials, silica, TOPAS, and Zionex are often used in photonic crystal fibers (PCFs). Additionally, it is noteworthy that most photonic crystal fibers (PCFs) operate inside the Terahertz frequency range.

Tuberculosis is an infectious respiratory ailment caused mainly by the Mycobacterium tuberculosis. It ranks among the top ten fatal diseases globally and first among contagious diseases [14]. This infection's transmission occurs by inhaling aerosols, resulting in a granulomatous infection in the lower respiratory tract [15]. So, significant and continuous efforts are required to develop, evaluate, and potentially manufacture and distribute various technologies, sensors, and equipment within the medical domain to assist individuals facing these challenges. More than that, if these efforts are focused on early detecting systems, the results will be excellent and valuable. Early spotting methods need to meet several conditions. High sensing precision, minimal operational losses, low power consumption, tiny devices, and rapid reaction times are only a few examples.

Either the old tests for tuberculosis are wrong, or they take too long to finish [16], [17]. There is also no quick and accurate way to tell the difference between current and dormant TB cases. The diagnostic methods commonly employed for tuberculosis detection encompass the utilization of chest radiography, tuberculin skin testing, and the assessment of interferon-gamma release assays in the bloodstream. Each one has its flaws. For example, a chest X-ray alone can't tell much, and the TST isn't very detailed or reliable. You can improve these methods by combining them with other methods, like artificial intelligence [18], [19]. This will make them much more helpful. This work aims to fill that gap by creating a new type of photonic crystal fiber sensor that uses the unique interactions between light and matter to allow label-free, sensitive optical testing of biomarkers for tuberculosis, which can improve patient results.

The paramount accomplishment of the sensor based on photonic crystal fibers (PCF) lies in its capacity to manipulate optical characteristics through the deliberate adjustment of the air hole pattern, size, and shape. Furthermore, sensors based on photonic crystal fibers (PCFs) exhibit many advantageous characteristics, including but not limited to heightened sensitivity, compact dimensions, cost-effectiveness, resilience, and enhanced adaptability. These attributes enable PCF-based sensors to offer efficacious resolutions for various environmental and industrial challenges [20].

Many studies have examined Photonic Crystal Fiber (PCF) types and structures for various sensing tasks. Singh and Kaur [21] introduced a circular photonic crystal fiber (PCF) design featuring a solid core to identify different blood components. The researchers investigated the sensitivity response of several substances, including water, plasma, white blood cells (WBCs), red blood cells (RBCs), and hemoglobin. The obtained sensitivity percentages for these substances were 55.09%, 54.05%, 53.72%, 56.05%, and 66.47% respectively. The researchers also examined the phenomenon of confinement loss and obtained the following values: 8.13×10−9 (dB/m) for water, 4.87×10−7 (dB/m) for plasma, 1.81×10−8 (dB/m) for white blood cells (WBCs), 4.07×10−7 (dB/m) for red blood cells (RBCs), and 1.19×10−8 (dB/m) for hemoglobin. However, the researchers could not get a substantial sensitivity response for all analytes. Furthermore, the sensor employed silica as its background material, and a comprehensive analysis of its properties was conducted using optical wavelengths. Bulbul et al. [22] recently published a study on a sensor design utilizing photonic crystal fiber (PCF) to detect formalin. The suggested detection methodology entailed the introduction of a formalin solution as the analyte into the PCF core. The study involved the implementation of numerical simulations to analyze and describe the optical behavior within the terahertz frequency range spanning from 1 to 2 THz. The sensor demonstrated a peak relative sensitivity of around 77.71% when operating at a frequency of 1.8 THz. Significantly, the loss due to confinement was diminished to insignificant levels beyond the frequency of 1.3 THz. A group of researchers [23] created a circular photonic crystal fiber (PCF) with a solid center that can find different parts of blood. Researchers looked into other chemicals' sensitivity, such as hemoglobin, red blood cells (RBCs), white blood cells (WBCs), plasma, and water. In that order, the sensitivity rates found for these substances were 80.93%, 80.56%, 80.13%, 79.91%, and 79.39%. The researchers also looked into confinement loss and found that for the same analytes and 1.5 THz frequency, the following values were gained: 1.23×10-11 dB/m, 8.63×10-12 dB/m, 4.93×10-12 dB/m, 2.93×10-12 dB/m, and

1.13×10-12 dB/m. Another group of researchers [24] proposed a decagonal Solid Core Photonic Crystal Fiber (SC-PCF) sensor for efficiently detecting blood cells. The background material deployed in the PCF is TOPAS, and the model is subjected to numerical analysis inside the terahertz frequency range. This sensor achieved the highest sensitivity in the terahertz spectrum for glucose, plasma, WBC, and RBC at 84.55%, 85.09%, 85.62%, and 87.68%, respectively. Additionally, all test analytes exhibited a confinement loss of around 10-9 dB/m. Finally, Nazmi et al. [25] recently published a study on a photonic crystal fiber (PCF) sensor designed to detect and differentiate between different tuberculosis strains. The complex (PCF) sensor structure, including circular and rectangular holes in a hybrid pattern, operates in the terahertz (1 THz – 2.4 THz) regimes. The performance parameters that were optimized numerically consisted of a relative sensitivity of 90.6%, an exceptionally low confinement loss of 3.13× 10-9 dB/m

Earlier research into terahertz photonic crystal fiber (PCF) sensors needed complex microstructural designs [21]–[25]. This work uses a basic, easy-to-fabrication PCF construction to make ultrasensitive tuberculosis detection possible. It is unnecessary to have a complex structure when only one hollow core surrounded by a hexagonal photonic crystal lattice is used. In previous designs[22]–[25], TOPAS and Zeonex were often used as background material, but this biosensor can be made entirely of silica, lowering production costs. Using optical wavelength bands instead of unique terahertz frequencies makes the external optics system easier. Surprisingly, this simple PCF design combined with well-known materials in standard spectral windows leads to a high increase in sensitivity compared to previous setups while also getting low confinement loss measures.

2. Model design

Fig 1 illustrates the cross-sectional structure of the proposed photonic crystal fiber (PCF) sensor. The sensing analyte is injected into one hollow core in the construction shown. Dc shows the width of this channel. Five rings of circular air holes arranged in a hexagonal pattern are suggested in the cladding area to make a dielectric area around the core. The letter d serves as a designation for each air hole's diameter. Pitch, written as p, is the smallest space between two air hole rings that come after each other. The suggested PCF sensor is designed with a total diameter of the fiber of 48 µm, a cladding composed of air holes with a diameter of d = 2.8 µm, and a pitch distance of p = 3 µm. The center of the fiber has a circular hole with a diameter of dc = 8 µm, which can be filled with various liquid analytes.

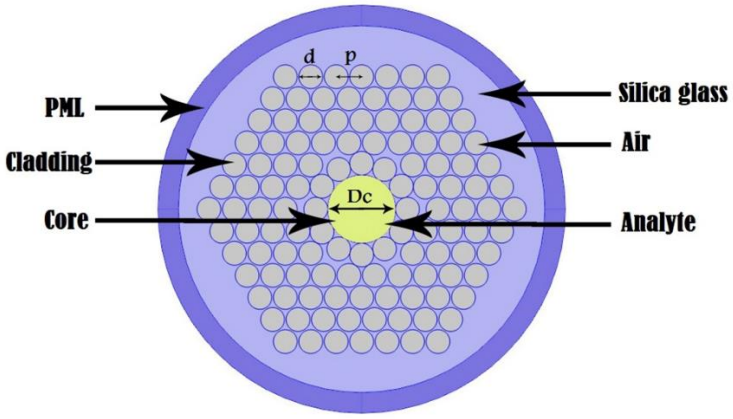

Fig. 1. Cross-section of the proposed PCF biosensor

While the light beam moves through the fiber's core, some of it veers off course and moves toward the outside of the waveguide. After that, back reflection sends some of the light from above to the core. A circle perfectly matched layer (PML) border condition was added to prevent this. The main goal of this condition is to absorb the light that comes in successfully. Fused silica was used as the base material for the suggested biosensor because it has better visual qualities than other materials. The Sellmeier equations [21], [26], [27] are used to find the

background material's refractive index (RI). The Sellmeier factors are ($B_1 = 0.696166300, B_2 = 0.407942600, B_3 = 0.897479400, C_1 = 0.00467914826, C_2 = 0.0135120631, C_3 = 97.9340025$).

$$n_{eff}(\lambda) = \sqrt{1 + \frac{B_1\lambda^2}{\lambda^2 - C_1} + \frac{B_2\lambda^2}{\lambda^2 - C_2} + \frac{B_3\lambda^2}{\lambda^2 - C_3}} \quad (1)$$

3. Methodology

A simulation was run using COMSOL Multiphysics software version 5.5 and the full-vector finite element method (FV-FEM) to determine how well the suggested PCF design worked. A finer meshing type was used to ensure the design was mapped accurately. This produced a mesh with 520 vertex elements, 4991 edge elements, and 45,588 triangular elements. It was found that the mesh had 387 834 degrees of freedom. Utilizing this mesh pattern results in an increased quantity of domain and boundary elements at the core-cladding junctions, which is advantageous for conducting a thorough and efficient model analysis. Fig 2 depicts the finer mesh view.

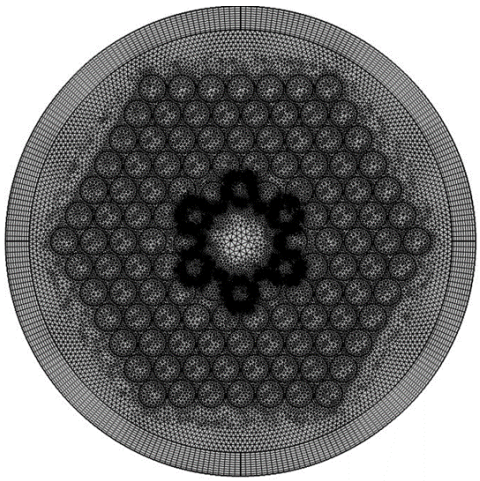

Fig. 2. Finer mesh of the proposed PCF biosensor.

The suggested photonic crystal fiber (PCF) design's optical properties were examined for its uses and how well it would work. Its optical features were looked at to determine what the design could be used for. These included effective refractive index (n_{eff}), relative sensitivity, confinement loss, and effective area (A_{eff}). All of these parameters affect how well a biosensor works. For PCF-based devices to work, the light has to travel mainly through the core area and stay close to the core.

The PCF sensor's relative sensitivity (S) measures how well it can find analytes. This is done by counting how much light moves through the gap between the analyte's refractive index and the medium around it. To figure out relative sensitivity, use the equation [28]:

$$S = \frac{n_r}{n_{eff}} \times f \quad (2)$$

The equation presented above elucidates the correlation between the refractive index (n_r) of the detected sample, the modal refractive index (n_{eff}), and the power fraction (f) of the seen sample. The power fraction is defined as the quotient of the power within a chemically loaded region to the total capacity across the entire fiber and is computed using integration. This statistic quantifies the energy transported via the photonic crystal fiber (PCF) at a specific place. The utilization of Poynting's theorem derives the equation in question [29].

$$f = \frac{(sample)\int Re\left(E_x H_y - E_y H_x\right)dxdy}{(total)\int Re\left(E_x H_y - E_y H_x\right)dxdy} \times 100 \quad (3)$$

The guided mode's transverse electric and magnetic fields are shown as E_x, E_y, and H_x, H_y, respectively. The integral in the numerator of the equation covers the part of the fiber where the analyte is, which is the fiber's core. The integral in the denominator, on the other hand, covers the whole fiber.

The PCF design shows light leaking from the core into the cladding area as confinement loss. This loss of control is caused by the way the fiber is built. To find the confinement loss, you need to figure out the imaginary part of the complex effective index. This can be done by using the following equation [29], [30]:

$$L_c = 8.686 \times \frac{2\pi f}{c} Im\left(n_{eff}\right)(\mathrm{dB/cm}) \quad (4)$$

The operation frequency f, the speed of light c, and the imaginary part of the effective refractive index $\mathrm{Im}(n_{eff})$ are all used in this equation to figure out the confinement loss in the PCF.

The transverse electric field vector of the whole cross-sectional area of the PCF is used to find the effective area of the fiber core, A_{eff}. The effective mode area is connected to the effective area of the fiber core. The effective area of the fiber core is the part of the core that can move light. This is the equation that is used to find the fiber core's useful area [29], [31]:

$$A_{eff} = \frac{\left(\iint_{-\infty}^{\infty} |E|^2 dxdy\right)^2}{\iint_{-\infty}^{\infty} |E|^4 dxdy} \quad (5)$$

where E is the vector of the transverse electric field. Systems that send data at high bit rates need effective mode areas that are big.

4. Results and Discussion

The precise measurement of the refractive index of healthy cells and cells infected with various types of mycobacterium tuberculosis will provide valuable insights for developing the sensor. Table 1 lists the refractive indices that may be used to identify the status of the sample, including those that can be discovered in both healthy and infected mycobacterium tuberculosis samples [32]–[34]. According to the information provided in Table 1, each measurement of the refractive index will be linked to a different kind of sample that is either normal or diseased.

Table 1 Refractive indices of cells infected with several tuberculosis strains.

Samples		Refractive Index (RI)
Healthy Plasma Cells	**HPC**	1.351
Cells that have been infected with many strains of TB	**TB1**	1.343
	TB2	1.345
	TB3	1.347
	TB4	1.348

Consistent with theoretical assumptions, experiments show that the effective refractive index of the studied materials declines with increasing operating wavelength. Fig 3 shows that the suggested PCF setup follows the same pattern. Small electromagnetic waves undergo this process when traveling through an area with a high refractive index, causing the effective refractive index to decrease. Healthy Plasma Cells (HPC) was found to have the highest refractive index of all the analytes tested, whereas infected mycobacterium tuberculosis plasma samples had the lowest.

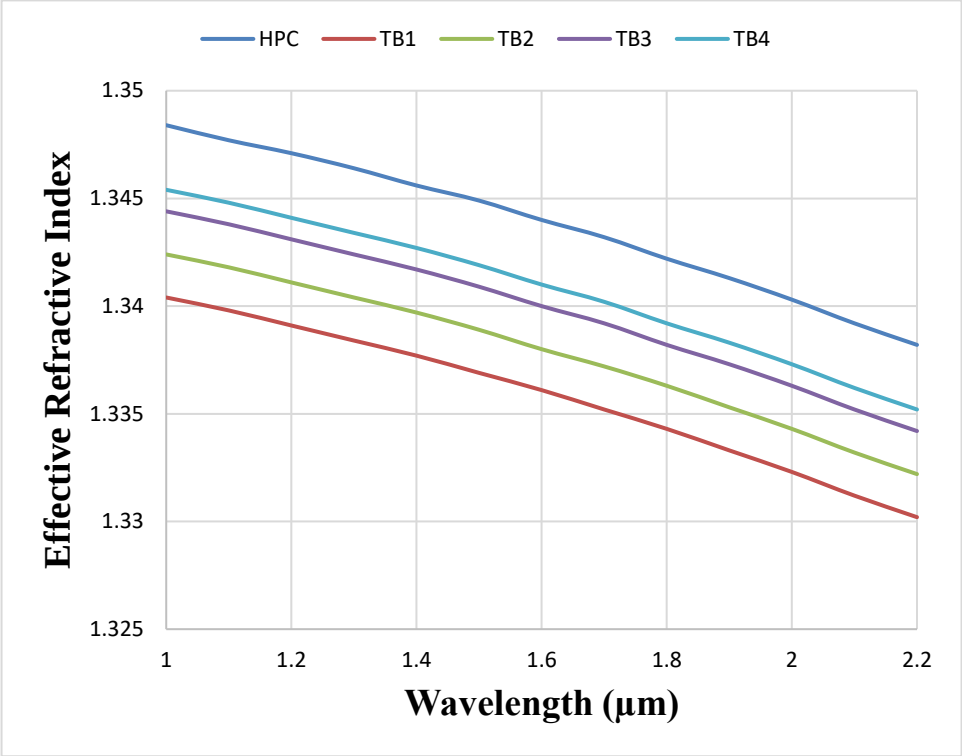

Fig. 3. Effective refractive index variation with wavelength of proposed biosensor for normal and tuberculosis-infected samples

Infected cell samples exhibit a wide range of relative sensitivity values between 1 µm and 2.2 µm, as seen in Fig 4. As previously mentioned, the formula for determining relative sensitivity is given in Eq. 5. All samples show an increase in relative sensitivity between 1 and 2 µm. All infected samples show a frequency between 2 and 2.2 µm, which is remarkably stable. The best wavelength for all samples is 2 µm because relative sensitivity is constant at wavelength 2 µm.

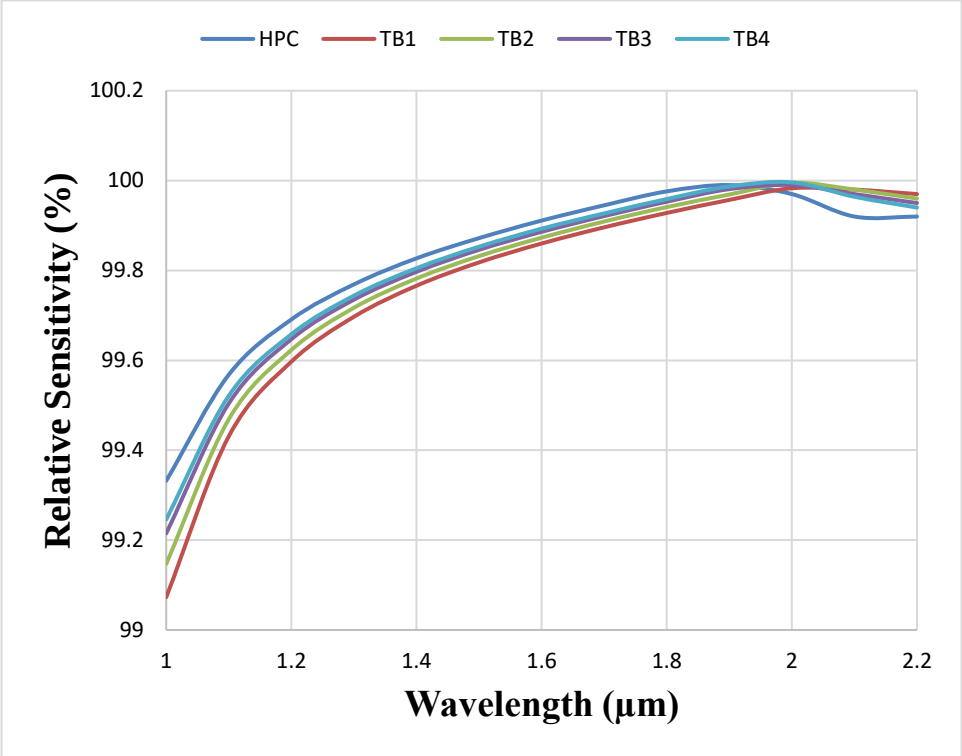

Fig. 4. Sensitivity variation with wavelength of proposed biosensor for normal and tuberculosis-infected samples

The phenomenon of confinement loss becomes increasingly evident as the wavelength rises, mainly attributed to light leakage from the core to the cladding. However, the core's clever design and the presence of air holes in the cladding effectively limit the loss of light signal, leading to minimum confinement loss. The confinement loss values, measured at a wavelength of 2 µm, are determined to be as follows: The concentration of a certain substance in healthy plasma is 2.26×10^{-11} dB/m. However, for samples infected with distinct forms of tuberculosis (TB1, TB2, TB3, and TB4), the concentrations are 3.93×10^{-11} dB/m, 6.02×10^{-11} dB/m, 7.33×10^{-11} dB/m, and 8.66×10^{-11} dB/m, respectively. Fig 5 showcases the confinement loss versus wavelength.

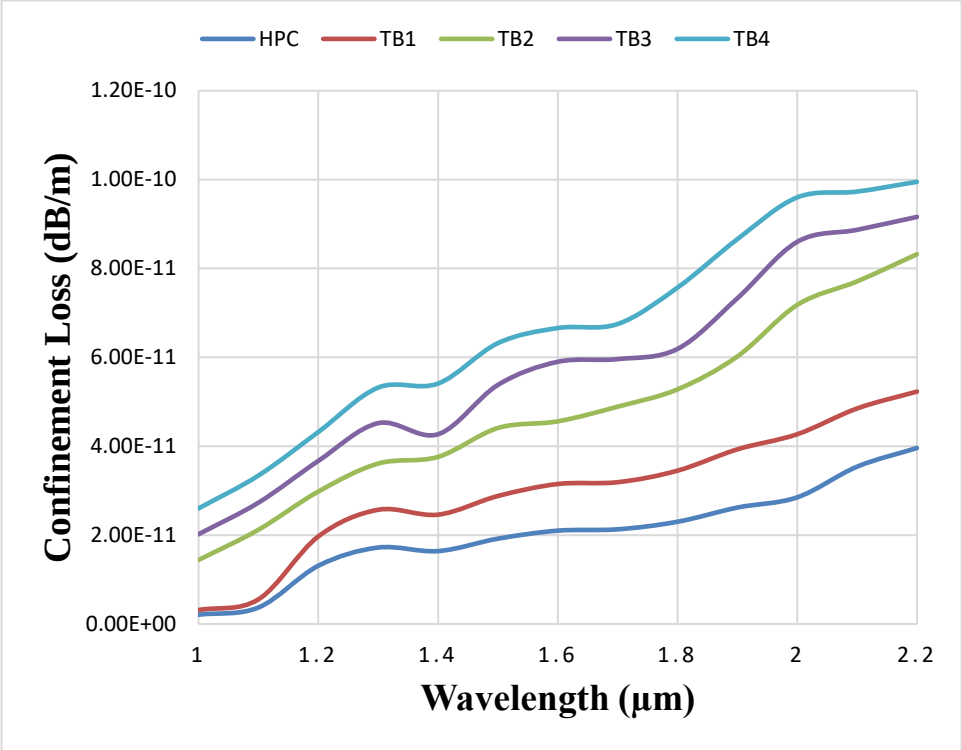

Fig. 5. Variation of confinement loss versus wavelength of proposed biosensor for normal and tuberculosis-infected samples

Fig 6 depicts the variation in the proposed photonic crystal fiber (PCF) effective area concerning the wavelength. The effective area may be defined as a measurable quantity that characterizes the transverse electric fields, demonstrating a propensity to increase as the operating wavelength increases. The figure shows a gradual increase in effective area with the increase in wavelength for all samples. An effective area of roughly 38 μm^2 is attained for all concentrations of sulfuric acid at a wavelength of 2 µm. The efficacy of the Photonic Crystal Fiber (PCF) is contingent upon its effective area, with a larger effective area often resulting in heightened sensor sensitivity.

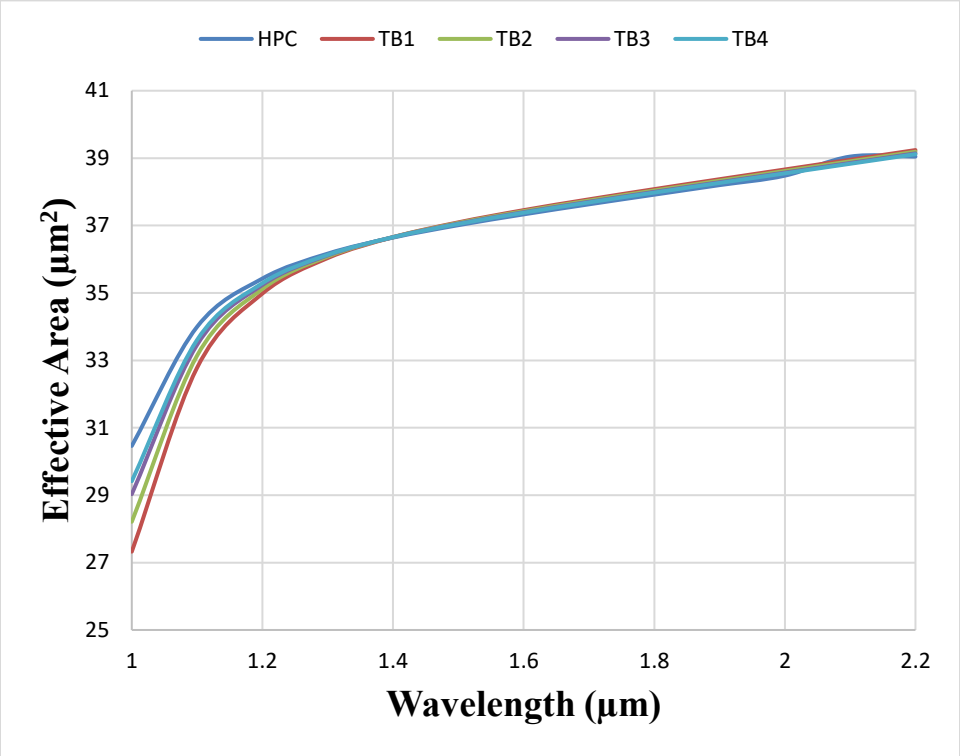

Fig. 6. Variation of effective area versus wavelength of proposed biosensor for normal and tuberculosis-infected samples

Fig 7 illustrates the electric field distribution for healthy blood plasma and samples contaminated with four different strains of tuberculosis when seen at the appropriate wavelength of 2 μm. The mode profiles demonstrate how light interacts inside the core region, with the mode field entirely confined to the core area of the mode profile.

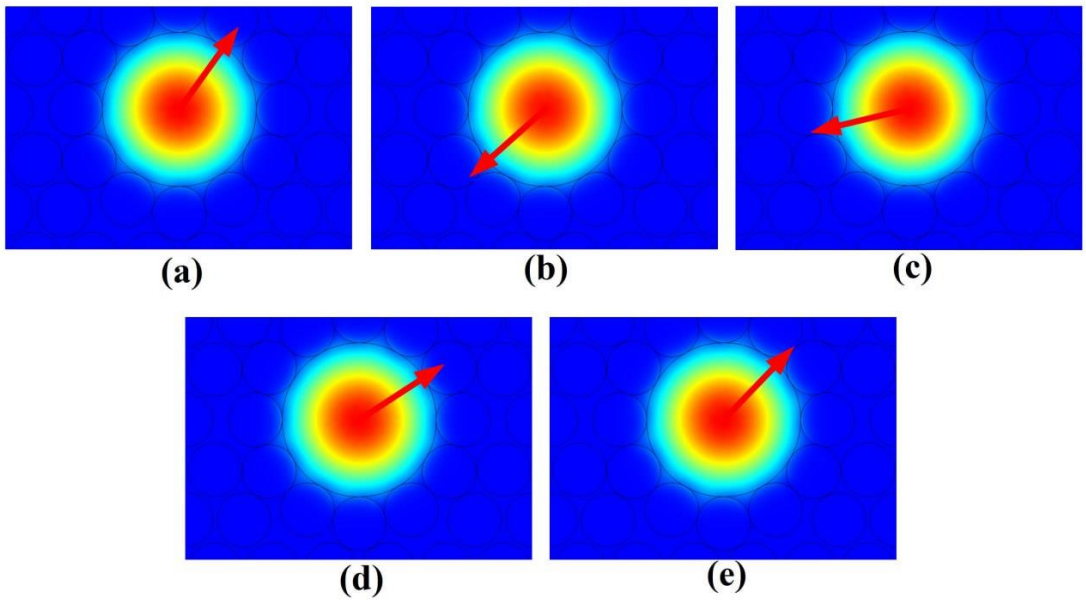

Fig. 7: Electric field distribution at 2 μm for different plasma samples: (a) HPC, (b) TB1, (c) TB2, (d) TB3, (e) TB4

Table 2 compares the proposed PCF with previously analyzed PCF biosensors, stressing the increased performance of the suggested PCF in terms of confinement loss and relative sensitivity. According to the statistics in the table, the suggested PCF biosensor is the most sensitive of the sensors considered. Furthermore, it exhibits the remarkable property of decreased confinement loss.

Table 2 Contrast between the proposed PCF and previously studied PCF biosensors

Biosensor	Sensitivity (%)	Confinement Loss (dB/m)
Reference [21]	66.47	$\sim 10^{-9}$
Reference [22]	77.71	-
Reference [23]	80.93	$\sim 10^{-12}$
Reference [24]	87.68	$\sim 10^{-9}$
Reference [25]	90.60	$\sim 10^{-9}$
This work	99.99	$\sim 10^{-11}$

5. Conclusions

Early identification and discovery of tuberculosis cases are essential for better patient results and fewer people who get the disease. A novel photonic crystal fiber (PCF) detector is described here that can distinguish between healthy blood plasma and samples contaminated with four strains of tuberculosis. A lot of computers planning and modeling was done to create a PCF structure aiming activity in the optical wavelength range (1 µm - 2.2 µm). The simulations proved that the biosensor could correctly tell the difference between types of plasma, with a maximum relative sensitivity of 99.9%. Notably, a very low confinement loss of 10-11 dB/m was achieved. The sensor's high performance was helped by its small effective area of only 38 µm2, which made it more sensitive than current optical biosensors. Comparative studies proved that the suggested biosensor had advanced features, with sensitivity and loss measures that are better than current photonic platforms for screening for tuberculosis. This work uses label-free optical biosensing to set up a framework for customized photonic engineering to meet essential goals in fast testing and preventing infectious diseases.

Acknowledgement: This is an optional section.

Conflict of Interest: The authors declare that there are no conflicts of interest associated with this research project. We have no financial or personal relationships that could potentially bias our work or influence the interpretation of the results.

References

[1] T. P. Hansen et al., "Highly birefringent index-guiding photonic crystal fibers," IEEE Photonics Technology Letters, vol. 13, no. 6, pp. 588-590, Jun. 2001. https://doi.org/10.1109/68.924030

[2] W. H. Reeves, J. C. Knight, P. S. J. Russell, and P. J. Roberts, "Demonstration of ultra-flattened dispersion in photonic crystal fibers," Opt Express, vol. 10, no. 14, pp. 609-613, 2002. https://doi.org/10.1364/OE.10.000609

[3] A. Habib, S. Anower, and R. Hasan, "Ultrahigh birefringence and extremely low loss slotted-core microstructure fiber in terahertz regime," Current Optics and Photonics, vol. 1, no. 6, pp. 567-572, 2017.

[4] A. M. R. Pinto and M. Lopez-Amo, "Photonic crystal fibers for sensing applications," J Sens, vol. 2012, 2012. https://doi.org/10.1155/2012/598178

[5] M. Hossain, E. Podder, A. Adhikary, and A. Al-Mamun, "Optimized hexagonal photonic crystal fibre sensor for glucose sensing," Adv Res, vol. 13, no. 3, pp. 1-7, 2018.
https://doi.org/10.9734/AIR/2018/38972

[6] B. Troia, A. Paolicelli, F. De Leonardis, and V. M. N. Passaro, "Photonic crystals for optical sensing: A review," Advances in Photonic Crystals, pp. 241-295, 2013.
https://doi.org/10.5772/53897

[7] H. K. Gahir and D. Khanna, "Design and development of a temperature-compensated fiber optic polarimetric pressure sensor based on photonic crystal fiber at 1550 nm," 2007.
https://doi.org/10.1364/AO.46.001184

[8] A.A. Rifat, K. Ahmed, S. Asaduzzaman, B.K. Paul, R. Ahmed, Development of photonic crystal fiber-based gas/chemical sensors, Computational Photonic Sensors (2019) 287–317.
https://doi.org/10.1007/978-3-319-76556-3_12

[9] T. Martynkien, M. Szpulak, and W. Urbanczyk, "Modeling and measurement of temperature sensitivity in birefringent photonic crystal holey fibers," Appl Opt, vol. 44, no. 36, pp. 7780-7788, 2005.
https://doi.org/10.1364/AO.44.007780

[10] W. J. Bock, J. Chen, T. Eftimov, and W. Urbanczyk, "A photonic crystal fiber sensor for pressure measurements," IEEE Trans Instrum Meas, vol. 55, no. 4, pp. 1119-1123, Aug. 2006.
https://doi.org/10.1109/TIM.2006.876591

[11] S. Asaduzzaman and K. Ahmed, "Proposal of a gas sensor with high sensitivity, birefringence and nonlinearity for air pollution monitoring," Sens Biosensing Res, vol. 10, pp. 20-26, 2016.
https://doi.org/10.1016/j.sbsr.2016.06.001

[12] S. Asaduzzaman, K. Ahmed, T. Bhuiyan, and T. Farah, "Hybrid photonic crystal fiber in chemical sensing," Springerplus, vol. 5, pp. 1-11, 2016.
https://doi.org/10.1186/s40064-016-2415-y

[13] M. J. B. M. Leon and M. A. Kabir, "Design of a liquid sensing photonic crystal fiber with high sensitivity, bireferingence & low confinement loss," Sens Biosensing Res, vol. 28, p. 100335, 2020.
https://doi.org/10.1016/j.sbsr.2020.100335

[14] J. Chakaya et al., "Global Tuberculosis Report 2020-Reflections on the Global TB burden, treatment and prevention efforts," International journal of infectious diseases, vol. 113, pp. S7-S12, 2021.
https://doi.org/10.1016/j.ijid.2021.02.107

[15] P. J. Quinn, B. K. Markey, M. E. Carter, W. J. Donnelly, and F. C. Leonard, Microbiologia veterinária e doenças infecciosas. Artmed Editora, 2005.

[16] F. A. Al-Zamel, "Detection and diagnosis of mycobac terium tuberculosis," Expert Review of Anti-Infective Therapy, vol. 7, no. 9. pp. 1099-1108, Nov. 2009.
https://doi.org/10.1586/eri.09.92

[17] S. K. Srivastava, C. J. M. Van Rijn, and M. A. Jongsma, "Biosensor-based detection of tuberculosis," RSC Adv, vol. 6, no. 22, pp. 17759-17771, 2016.
https://doi.org/10.1039/C5RA15269K

[18] S. Gull and S. Akbar, "Artificial intelligence in brain tumor detection through MRI scans: Advancements and challenges," Artificial Intelligence and Internet of Things, pp. 241-276, 2021.
https://doi.org/10.1201/9781003097204-10

[19] F. A. Al-Zamel, “Detection and diagnosis of Mycobacterium tuberculosis,” *Expert Review of Anti Infective Therapy*, 2009, 7(9): 1099–1108.
https://doi.org/10.1586/eri.09.92

[20] T. Zhang, Y. Zheng, C. Wang, Z. Mu, Y. Liu, and J. Lin, "A review of photonic crystal fiber sensor applications for different physical quantities," Appl Spectrosc Rev, vol. 53, no. 6, pp. 486-502, 2018.
https://doi.org/10.1080/05704928.2017.1376681

[21] N. A. Mohammed, O. E. Khedr, E.-S. M. El-Rabaie, and A. A. M. Khalaf, “High-sensitivity early detection biomedical sensor for tuberculosis with low losses in the terahertz regime based on photonic crystal fibre technology,” Photonic Sens., vol. 13, no. 2, 2023.
https://doi.org/10.1007/s13320-023-0675-z

[22] A. A. M. Bulbul, R. H. Jibon, S. K. Das, T. Roy, A. Saha, and M. B. Hossain, "PCF based formalin detection by exploring the optical properties in THz regime," Nanoscience & Nanotechnology-Asia, vol. 11, no. 3, pp. 314-321, 2021.
https://doi.org/10.2174/2210681210999200525171303

[23] K. Ahmed et al., "Refractive Index-Based Blood Components Sensing in Terahertz Spectrum," IEEE Sens J, vol. 19, no. 9, pp. 3368-3375, May 2019.
https://doi.org/10.1109/JSEN.2019.2895166

[24] A. Kumar, P. Verma, and P. Jindal, "Decagonal solid core PCF based refractive index sensor for blood cells detection in terahertz regime," Opt Quantum Electron, vol. 53, no. 4, Apr. 2021.
https://doi.org/10.1007/s11082-021-02818-x

[25] N. A. Mohammed, O. E. Khedr, E. S. M. El-Rabaie, and A. A. M. Khalaf, "High-Sensitivity Early Detection Biomedical Sensor for Tuberculosis With Low Losses in the Terahertz Regime Based on Photonic Crystal Fiber Technology," Photonic Sensors, vol. 13, no. 2, Jun. 2023.
https://doi.org/10.1007/s13320-023-0675-z

[26] A. M. Maidi et al., "Design and simulation of photonic crystal fiber for liquid sensing," Photonics, vol. 8, no. 1, pp. 1-14, Jan. 2021.
https://doi.org/10.3390/photonics8010016

[27] E. K. Akowuah, T. Gorman, H. Ademgil, S. Haxha, G. K. Robinson, and J. V. Oliver, "Numerical analysis of a photonic crystal fiber for biosensing applications," IEEE J Quantum Electron, vol. 48, no. 11, pp. 1403-1410, 2012.
https://doi.org/10.1109/JQE.2012.2213803

[28] M. Hossain, E. Podder, A. Adhikary, and A. Al-Mamun, "Optimized hexagonal photonic crystal fibre sensor for glucose sensing," Adv Res, vol. 13, no. 3, pp. 1-7, 2018.
https://doi.org/10.9734/AIR/2018/38972

[29] I. Yakasai, P. E. Abas, S. F. Kaijage, W. Caesarendra, and F. Begum, "Proposal for a quad-elliptical photonic crystal fiber for terahertz wave guidance and sensing chemical warfare liquids," Photonics, vol. 6, no. 3, 2019.
https://doi.org/10.3390/photonics6030078

[30] M. F. H. Arif, M. M. Hossain, N. Islam, and S. M. Khaled, "A nonlinear photonic crystal fiber for liquid sensing application with high birefringence and low confinement loss," Sens Biosensing Res, vol. 22, p. 100252, 2019.
https://doi.org/10.1016/j.sbsr.2018.100252

[31] I. K. Yakasai, P. E. Abas, S. Ali, and F. Begum, "Modelling and simulation of a porous core photonic crystal fibre for terahertz wave propagation," Opt Quantum Electron, vol. 51, no. 4, Apr. 2019.
https://doi.org/10.1007/s11082-019-1832-x

[32] S. A. Taya, M. G. Daher, I. Colak, and O. M. Ramahi, "Highly sensitive nano-sensor based on a binary photonic crystal for the detection of mycobacterium tuberculosis bacteria," Journal of Materials Science: Materials in Electronics, vol. 32, pp. 28406-28416, 2021.
https://doi.org/10.1007/s10854-021-07220-7

[33] A. H. Aly et al., "Novel biosensor detection of tuberculosis based on photonic band gap materials," Materials Research, vol. 24, 2021.
https://doi.org/10.1590/1980-5373-mr-2020-0483

[34] N. R. Ramanujam, S. K. Patel, N. Manohar Reddy, S. A. Taya, D. Vigneswaran, and M. S. Mani Rajan, "One-dimensional ring mirror-defect photonic crystal for detection of mycobacterium tuberculosis bacteria," Optik (Stuttg), vol. 219, Oct. 2020.
https://doi.org/10.1016/j.ijleo.2020.165097